



Centromere-Associated Female Meiotic Drive Entails Male Fitness Costs in Monkeyflowers

Lila Fishman, *et al.*

Science **322**, 1559 (2008);

DOI: 10.1126/science.1161406

**The following resources related to this article are available online at
www.sciencemag.org (this information is current as of December 4, 2008):**

Updated information and services, including high-resolution figures, can be found in the online version of this article at:

<http://www.sciencemag.org/cgi/content/full/322/5907/1559>

Supporting Online Material can be found at:

<http://www.sciencemag.org/cgi/content/full/322/5907/1559/DC1>

This article **cites 23 articles**, 2 of which can be accessed for free:

<http://www.sciencemag.org/cgi/content/full/322/5907/1559#otherarticles>

This article appears in the following **subject collections**:

Evolution

<http://www.sciencemag.org/cgi/collection/evolution>

Information about obtaining **reprints** of this article or about obtaining **permission to reproduce this article** in whole or in part can be found at:

<http://www.sciencemag.org/about/permissions.dtl>

cause intracellular perfusion with 4 mM MgATP significantly protected against Pxl activation; current density was -30.2 ± 8.6 pA/pF ($n = 3$) with 1 mM MgATP and -9.4 ± 3.7 pA/pF ($n = 5$) with 4 mM MgATP. We recently reported that Pxl is opened by ischemia (1) and that the timing of this opening appears to follow the anoxic depolarization (23) in a manner analogous to Pxl activation after NMDAR stimulation. Therefore, Pxl not only appears to be involved in neuronal dysfunction during ischemia but also plays a role in the potentiation of seizure-like activity. These unique ion channels should therefore be considered important targets for the treatment of neurological disorders such as epilepsy and stroke.

References and Notes

1. R. J. Thompson, N. Zhou, B. A. MacVicar, *Science* **312**, 924 (2006).
2. S. Locovei, L. Bao, G. Dahl, *Proc. Natl. Acad. Sci. U.S.A.* **103**, 7655 (2006).
3. G. Zoidl *et al.*, *Neuroscience* **146**, 9 (2007).

4. Q. X. Chen, K. L. Perkins, D. W. Choi, R. K. S. Wong, *J. Neurosci.* **17**, 4032 (1997).
5. J. A. Connor, R. J. Cormier, *J. Neurophysiol.* **83**, 90 (2000).
6. M. Tymianski, M. P. Charlton, P. L. Carlen, C. H. Tator, *J. Neurosci.* **13**, 2085 (1993).
7. Materials and methods are available as supporting material on Science Online.
8. R. Bruzzone, S. G. Hormuzdi, M. T. Barbe, A. Herb, H. Monyer, *Proc. Natl. Acad. Sci. U.S.A.* **100**, 13644 (2003).
9. P. Pelegrin, A. Surprenant, *EMBO J.* **25**, 5071 (2006).
10. Single-letter abbreviations for the amino acid residues are as follows: A, Ala; C, Cys; D, Asp; E, Glu; F, Phe; G, Gly; H, His; I, Ile; K, Lys; L, Leu; M, Met; N, Asn; P, Pro; Q, Gln; R, Arg; S, Ser; T, Thr; V, Val; W, Trp; and Y, Tyr.
11. L. Bao, S. Locovei, G. Dahl, *FEBS Lett.* **572**, 65 (2004).
12. C. Virginio, A. MacKenzie, R. A. North, A. Surprenant, *J. Physiol.* **519**, 335 (1999).
13. D. C. Spray, Z.-C. Ye, B. R. Ransom, *Glia* **54**, 758 (2006).
14. P. Pelegrin, A. M. Surprenant, *EMBO J.* **25**, 5071 (2007).
15. S. Panuela *et al.*, *J. Cell Sci.* **120**, 3772 (2006).
16. Y. Huang, J. B. Grinspan, C. K. Abrams, K. S. Scherer, *Glia* **55**, 46 (2007).
17. H. Walthers, J. D. C. Lambert, R. S. G. Jones, U. Heinemann, B. Hamon, *Neurosci. Lett.* **69**, 156 (1986).
18. J. P. Dreier, U. Heinemann, *Neurosci. Lett.* **119**, 68 (1990).

19. A. Nimmerjahn, F. Kirchhoff, J. N. D. Kerr, F. Helmchen, *Nat. Methods* **1**, 31 (2004).
20. E. A. Waxman, D. R. Lynch, *Neuroscientist* **11**, 37 (2005).
21. M. V. L. Bennett, A. Pereda, *Brain Cell Biol.* **35**, 5 (2007).
22. T. A. Vander Jagt, J. A. Connor, C. W. Shuttleworth, *J. Neurosci.* **28**, 5029 (2008).
23. T. H. Murphy, P. Li, K. Betts, R. Liu, *J. Neurosci.* **28**, 1756 (2008).
24. This work was supported by grants to B.A.M. from the Heart and Stroke Foundation of British Columbia, to B.A.M. or J.F.M. (15514) from the Canadian Institutes of Health Research, and by a grant from the Canadian Stroke Network to B.A.M., J.F.M., and R.J.T. B.A.M. holds a Canada Research Chair (Tier 1) in Neuroscience. The authors kindly acknowledge Y. T. Wang for critical reading of the manuscript and S. Panuela and D. Laird for generously providing the anti-Pxl antibody.

Supporting Online Material

www.sciencemag.org/cgi/content/full/322/5907/1555/DC1
Materials and Methods

Figs. S1 to S3

References

27 August 2008; accepted 29 October 2008

10.1126/science.1165209

Centromere-Associated Female Meiotic Drive Entails Male Fitness Costs in Monkeyflowers

Lila Fishman* and Arpiar Saunders†

Female meiotic drive, in which paired chromosomes compete for access to the egg, is a potentially powerful but rarely documented evolutionary force. In interspecific monkeyflower (*Mimulus*) hybrids, a driving *M. guttatus* allele (*D*) exhibits a 98:2 transmission advantage via female meiosis. We show that extreme interspecific drive is most likely caused by divergence in centromere-associated repeat domains and document cytogenetic and functional polymorphism for drive within a population of *M. guttatus*. In conspecific crosses, *D* had a 58:42 transmission advantage over nondriving alternative alleles. However, individuals homozygous for the driving allele suffered reduced pollen viability. These fitness effects and molecular population genetic data suggest that balancing selection prevents the fixation or loss of *D* and that selfish chromosomal transmission may affect both individual fitness and population genetic load.

In the female meioses of both plants and animals, all but one of the meiotic products generally degenerate (1). This asymmetry of cell fate can allow homologous chromosomes to compete for inclusion in the single surviving egg or megaspore, a process termed “female meiotic drive” (1–4). Female meiotic drive may explain the rapid diversification of centromeres, the DNA-protein complexes that mediate chromosomal segregation (5), and may promote speciation through the evolution of hybrid incompatibilities (5) and karyotypic rearrangements (6). Because nondisjunction during chromosomal competition can cause infertility (2, 5), female meiotic drive may also contribute to genetic variation for reproduc-

tive fitness within populations (7), a central issue in evolutionary biology (8–12) and human health. Despite its potential importance as an evolutionary force, little is known about female meiotic drive in natural populations.

The female meiotic-drive locus in *Mimulus* (*D*) exhibits extreme non-Mendelian segregation through female meiosis in hybrids between *M. guttatus* (IM62 inbred line) and its close relative *M. nasutus* (SF inbred line), which is predominantly self-fertilizing (13, 14). As seed parents, interspecific heterozygotes transmit >98% *M. guttatus* (IM62) alleles at markers tightly linked to *D*, and there is no evidence of postmeiotic mechanisms of transmission ratio distortion (13). Near-complete transmission bias via female meiosis suggests that *D* is the functional centromere of the chromosome corresponding to the linkage group [linkage group 11 (LG11)] on which it is located (13), because only the centromere (and linked loci) can attain >83.3% transmission via

female drive (15). To test this inference, we cytogenetically mapped *D* in *M. guttatus*, *M. nasutus*, and interspecific hybrids (Fig. 1) (SOM text). Because plant centromeres generally consist of megabases of tandemly repetitive DNA with individual repeats 150 to 1000 base pairs (bp) in length (16, 17), we searched the *M. guttatus* (IM62 line) 6× draft whole-genome sequence [Mimulus Genome Project, U.S. Department of Energy (DOE) Joint Genome Institute] for repeats with those features. A probe for the most common class of repeat found, 728 bp in length (Cent728; fig. S1), hybridized to a single narrow band near the center of each IM62 metaphase chromosome (Fig. 1A and fig. S2A). However, a single pair of homologous chromosomes exhibited two unusually large regions of hybridization (arrows; Fig. 1A and fig. S2A). A probe for the *CycA* genetic marker tightly linked to *D* (13) localized between the large Cent728 arrays on this chromosome (Fig. 1B and fig. S2B), demonstrating that this distinctive chromosomal structure (henceforth, C11.2) corresponds to the driving region of IM62 LG11. The region of Cent728 hybridization on each non-C11.2 chromosome was flanked by arrays of typically pericentromeric retrotransposons (Fig. 1C and fig. S2C) (18). This pattern suggests that Cent728 is, if not the centromere-specifying DNA repeat, a marker for centromeric chromosomal regions. Although we cannot yet determine whether the molecular mechanism of *Mimulus* drive is strictly centromeric (5) and whether the duplication and expansion of Cent728 arrays is causal, this association is consistent with the genetic evidence for centromeric drive (13, 15).

We examined metaphase chromosomes from nearly isogenic lines (NILs) containing heterozygous introgressions of *M. guttatus* *D* in a largely *M. nasutus* genetic background (13). Both strong Cent728 arrays from IM62 C11.2 appear present in the NILs (Fig. 1D and fig. S2D), which

Division of Biological Sciences, University of Montana, Missoula, MT 59812, USA.

*To whom correspondence should be addressed. E-mail: lila.fishman@mso.umt.edu

†Present address: Program in Neuroscience, Harvard Medical School, Boston, MA 02115, USA.

indicates that they were transmitted as a single genetic unit over five generations of recombination (there is a single weak Cent728 array on LG11 in the SF *M. nasutus* parent; fig. S3). Thus, the two IM62 C11.2 arrays are inherited as a single genetic locus. The large physical size of the D locus is similar to that of the best-known female meiotic drive system, Ab10-knob in maize (19), but in that case the drive elements are DNA arrays (knobs) that segregate as genetic loci unlinked from the centromeric regions (20). In contrast, our data suggest that female meiotic drive in *Mimulus* results from competition between chromosomal homologs divergent in centromere-associated repetitive DNA arrays. Regardless of its molecular mechanism, *Mimulus* drive differs from maize drive in its genomic location relative to centromeres (19–21) and thus provides a comparative model for understanding selfish chromosomal evolution.

To investigate drive within *M. guttatus*, we examined Cent728 hybridization to chromosomes from inbred lines from the Iron Mountain *M. guttatus* population (10). Some lines completely lacked the distinct C11.2 found in IM62 (Fig. 1E and fig. S2E), suggesting that the driving chromosome is structurally divergent from homologs within the same species. The Iron Mountain *M. guttatus* population is also polymorphic for heterospecific female meiotic drive, exhibiting discrete variation in segregation patterns at drive-linked markers (Fig. 2). Of the eight independently derived inbred lines test-crossed to *M. nasutus*, four exhibited strongly distorted segregation (*M. guttatus* allele transmitted at ~95% via F₁ female meiosis) similar to SF × IM62 hybrids (13, 14) and four exhibited Mendelian segregation. Thus, the driving allele (*D*) is at intermediate frequency in this *M. guttatus* population, along with nondriving alternative alleles (henceforth, *D*⁻). In addition, all three nondriving lines that we examined cytogenetically (including IM767; Fig. 1E and fig. S2E) lack the C11.2 arrays, supporting the inference that drive is associated with chromosomal divergence. This analysis also revealed that allelic variation at the microsatellite marker *aat356* (13, 14) was diagnostic for the drive genotype, because all five *D* lines shared the most common 180-bp allele [overall frequency = 37 out of 113 lines tested (33%)], whereas the four *D*⁻ lines were diverse and carried other alleles (*P* < 0.008; Fisher's exact test).

Because the driving *D* allele shows a near-complete transmission advantage over *M. nasutus* alleles via female meiosis (13), we tested whether it exhibits female drive against alternative conspecific genotypes by examining segregation in within-population test-crosses (SOM text). On average, *D* displayed a 58:42 conspecific transmission advantage via female meiosis ($\chi^2 = 4.45$, *P* = 0.035), but was transmitted in a Mendelian fashion via male meiosis ($\chi^2 = 0.51$, *P* = 0.475), resulting in 16% excess transmission of *D* via female function. Thus, although weaker than heterospecific drive, chromosomal competition appears to be a potent selective force within this

Fig. 1. Fluorescence in situ hybridization to *M. guttatus* lines and *M. nasutus* × *M. guttatus* hybrids (2*N* = 28). (A) IM62 *M. guttatus* metaphase karyotype showing a single band of Cent728 hybridization (green) on each chromosome and two large regions of Cent728 hybridization on one pair of chromosomes (arrows). (B) Colocalization of a genetic marker for drive (*CycA*; red; above) with C11.2 Cent728 arrays (merged; below). (C) Pachytene IM62 chromosomes with Cent728 (green; above) and flanking Mg_Copia69.2 retrotransposon arrays (red; overlay with Cent728 below). (D) C11.2 (arrow) from IM62 introgressed into *M. nasutus* genetic background. (E) IM767, an independent inbred line derived from the Iron Mountain *M. guttatus* population. Each image includes merged false-colored images of DNA-bound DAPI (4',6'-diamidino-2-phenylindole) (blue) with images of additional probes labeled in Alexa-Fluor (green) and/or Texas Red (red); component images are in fig. S2. Scale bar: 2 μ m.

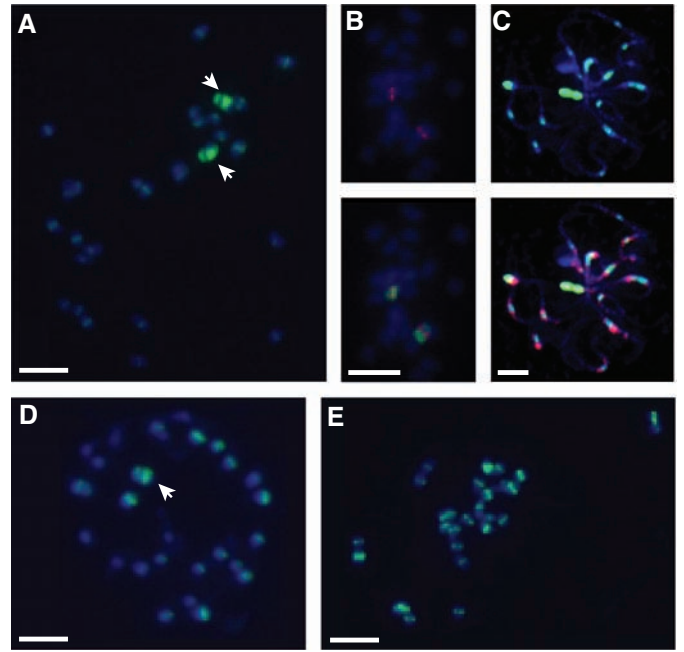


Fig. 2. Cumulative frequencies of *M. nasutus* homozygotes (NN; black), *M. guttatus* homozygotes (GG; white), and heterozygotes (NG; gray) for eight F₂ testcross families. By χ^2 tests (df = 2), four families (*D*) differed significantly (all *P* < 0.0001) from Mendelian segregation (1:2:1; NN:NG:GG), but not from the IM62 heterospecific drive expectation of 2:49:49 (*P* range: 0.12 to 0.40), whereas four families (*D*⁻) did not differ from Mendelian (*P* range: 0.34 to 0.97).

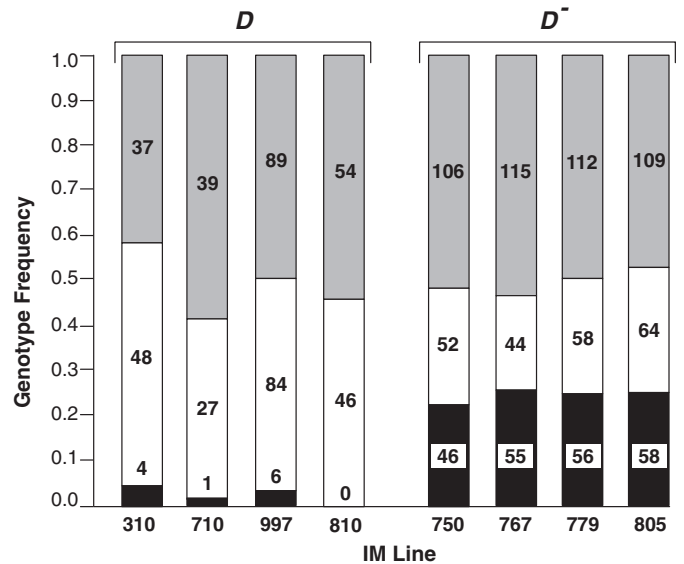
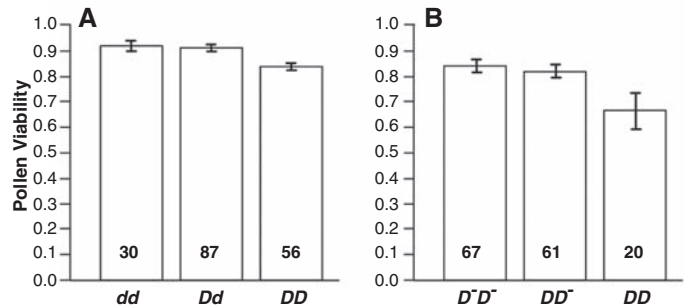


Fig. 3. Mean pollen viability (\pm SEM) of drive genotypes in (A) controlled heterospecific genetic background and environment and (B) wild *M. guttatus* plants. In both cases, the overall effect of *D* genotype was highly significant (one-way analysis of variance: *P* < 0.007) and *DD* homozygotes had significantly lower pollen viability than the other genotypes, which did not differ from each other. (A) Least squares means (LSMs) contrasts. *DD* versus other: *P* = 0.0003; *dd* versus *Dd*: *P* = 0.82. (B) LSMs contrasts. *DD* versus other: *P* = 0.0018; *D*⁻*D*⁻ versus *DD*⁻: *P* = 0.59.



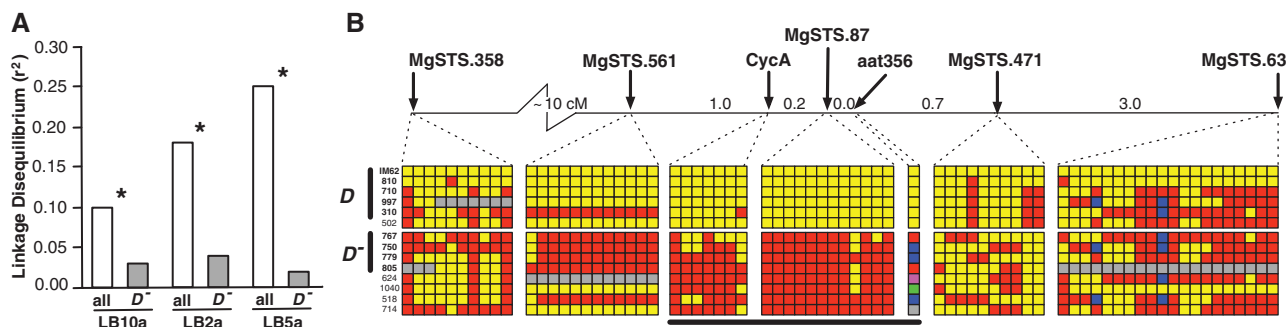


Fig. 4. (A) LD between *CycA* BAC microsatellites and *aat356* for all *D* and *D*⁻ lines ($N = 74$) and *D*⁻ lines only ($N = 45$). Asterisks indicate significant LD ($P < 0.05$). (B) Haplotype structure in the region flanking *D* (map location underlined) (13). Polymorphic sites (singletons excluded) are

shown (IM62 reference sequence: yellow; alternative alleles: blue, pink, green, and red; missing data: gray). The nine lines of known heterospecific drive phenotype (*D* and *D*⁻, respectively) are linked by vertical lines. See SOM text for methods. Full alignments are in fig. S4.

interbreeding population. The difference in strength between heterospecific and conspecific drive suggests that suppression of drive has evolved within *M. guttatus* or that genomic divergence between *M. guttatus* and *M. nasutus* intensifies chromosomal competition.

In the absence of countervailing selection, we would expect conspecific female drive to rapidly fix the driving *D* allele. Therefore, the observed polymorphism within the Iron Mountain *M. guttatus* population predicts that female meiotic drive has deleterious effects on individual fitness. We characterized the male fitness effects of heterospecific drive in the segregating progeny of a NIL with a heterozygous introgression at *D* (*Dd*, where *d* is the nondriving *M. nasutus* allele) (13). *DD* homozygotes had significantly reduced pollen viability relative to *Dd* heterozygotes and *dd* homozygotes (Fig. 3A). Because female meiotic drive in heterospecific (*Dd*) heterozygotes was near 100%, this suggests that even strongly biased chromosomal segregation may impose little direct cost via nondisjunction. This result supports the assumption of costs in the female meiotic drive model of centromere evolution (5), but rejects non-random chromosomal segregation in heterozygotes as the mechanism of drive costs in this system.

We assessed the effects of *D* on male fertility in wild *M. guttatus* plants at the Iron Mountain population (SOM text). The inferred genotype at the *D* locus strongly affected pollen viability in the field (Fig. 3B). *DD* homozygotes suffered a 20% reduction in pollen viability relative to other genotypic classes. Thus, deleterious recessive effects of *D* contribute to male fitness variation under natural conditions. Pollen inviability may be a pleiotropic effect of meiotic interactions between paired C11.2 homologs that cause nondisjunction or may reflect hitchhiking at a locus linked to *D*, because the C11.2 region contains expressed genes (SOM text).

The opposition of female meiotic drive and associated male fertility costs may produce a true balanced polymorphism in *M. guttatus*. In a random mating population, selection against a female meiotic drive allele in homozygous males must be approximately greater than twice its advantage in heterozygous females to prevent its fixation (Eq.

S1). Given the measured male fertility cost of ~0.20 to *D* homozygotes, any female-specific transmission ratio distortion below 60:40 should result in a protected polymorphism. Our observation of a 58:42 transmission advantage for *D* is within this range, indicating that *D* cannot be lost and is unlikely to fix under current conditions.

Patterns of molecular polymorphism and linkage disequilibrium (LD) also suggest short-term balancing selection or an ongoing selective sweep by *D* (22). We estimated LD between the drive-diagnostic marker *aat356* and three highly polymorphic microsatellites (6 to 19 alleles each; table S2A) that are physically associated with *CycA* and located at least 45 kb from *aat356* (SOM text). Like *aat356*, these markers each had one or two alleles only found in *D* lines, leading to high pairwise LD with *aat356* across all lines analyzed ($N = 74$; Fig. 4A). This was due to the low polymorphism of the inferred *D* lines, because inferred *D*⁻ lines ($N = 45$) were diverse and exhibited no significant LD when analyzed separately. Sequencing of the nine lines of known drive phenotype confirmed the uniqueness of the driving haplotype and revealed that drive-specific LD extends up to 2 cM (Fig. 4B and fig. S4). Thus, the driving allele *D* is a single physically and genetically extensive haplotype associated with the C11.2 chromosomal structure. As in maize (21), structural differences between driving and nondriving haplotypes (which may cause variation in recombination rate) complicate the interpretation of molecular population genetic data. However, the extent and uniformity of the *D* haplotype are consistent with recent selfish spread via female meiotic drive.

We have shown that selfish chromosomal drive has brought an allele with unconditionally deleterious effects on individual fitness to high frequency in a primarily outcrossing wildflower population. This high frequency contrasts with the generally low frequency of male drive elements (23, 24), which generally achieve excess transmission via the postmeiotic disabling of gametes with alternative genotypes, often entailing high fitness costs in heterozygotes. Female meiotic drivers such as *D*, which take advantage of the intrinsic asymmetry of female meiosis and

may have primarily recessive costs, may spread to high frequency despite biologically significant effects. Biometric tests (10) have found more standing variation for pollen viability at Iron Mountain than predicted under mutation-selection balance models, and female meiotic drive by *D* may account for this unexpectedly high genetic load. By contributing to inbreeding depression for male fertility, *D* may play an important role in mating system and floral trait evolution in monkeyflowers.

Untangling the molecular mechanism and evolutionary origins of *Mimulus* drive remains a challenge, as we do not yet know whether *D* biases transmission by using the machinery of normal centromere function or via an alternative mechanism. Regardless of mechanism, however, it is clear that selfish chromosomal drive can be an important determinant of fitness variation within natural populations.

References and Notes

1. F. Pardo-Manuel de Villena, C. Sapienza, *Mamm. Genome* **12**, 331 (2001).
2. M. E. Zwick, J. L. Salstrom, C. H. Langley, *Genetics* **152**, 1605 (1999).
3. R. K. Dawe, E. N. Hiatt, *Chromosome Res.* **12**, 655 (2004).
4. G. Wu *et al.*, *Genetics* **170**, 327 (2005).
5. S. Henikoff, K. Ahmad, H. S. Malik, *Science* **293**, 1098 (2001).
6. F. Pardo-Manuel de Villena, C. Sapienza, *Genetics* **159**, 1179 (2001).
7. A. Daniel, *Am. J. Med. Genet.* **111**, 450 (2002).
8. R. C. Lewontin, *The Genetic Basis of Evolutionary Change* (Columbia Univ. Press, New York, 1974).
9. N. H. Barton, P. D. Keightley, *Nat. Rev. Genet.* **3**, 11 (2002).
10. J. K. Kelly, *Genetics* **164**, 1071 (2003).
11. T. Johnson, N. Barton, *Philos. Trans. R. Soc. London B* **360**, 1411 (2005).
12. B. Charlesworth, T. Miyo, H. Borthwick, *Genet. Res.* **89**, 85 (2007).
13. L. Fishman, J. H. Willis, *Genetics* **169**, 347 (2005).
14. L. Fishman, A. Kelly, E. Morgan, J. H. Willis, *Genetics* **159**, 1701 (2001).
15. H. S. Malik, *Trends Ecol. Evol.* **20**, 151 (2005).
16. J. Jiang, J. A. Birchler, W. A. Parrott, R. K. Dawe, *Trends Plant Sci.* **8**, 570 (2003).
17. J. C. Lamb, W. Yu, F. Han, J. A. Birchler, *Curr. Opin. Plant Biol.* **10**, 116 (2007).
18. A. Kumar, J. L. Bennetzen, *Annu. Rev. Genet.* **33**, 479 (1999).
19. J. A. Birchler, R. K. Dawe, J. F. Doebley, *Genetics* **164**, 835 (2003).
20. E. S. Buckler *et al.*, *Genetics* **153**, 415 (1999).
21. R. J. Mroczek, J. R. Melo, A. C. Luce, E. N. Hiatt, R. K. Dawe, *Genetics* **174**, 145 (2006).

22. D. Charlesworth, *PLoS Genet.* **2**, e64 (2006).
 23. K. G. Ardlie, *Trends Genet.* **14**, 189 (1998).
 24. K. A. Dyer, B. Charlesworth, J. Jaenike, *Proc. Natl. Acad. Sci. U.S.A.* **104**, 1587 (2007).
 25. We thank J. H. Willis, J. K. Kelly, J. Birchler, D. Charlesworth, H. Malik, C. Barr, V. Ezenwa, D. Emlen, and S. Miller for critical comments; J. H. Willis, C. Wu, T. J. Vision, E. Ganko, L. Bridges, and J. K. Kelly for materials and communicating

unpublished results; and D. Pedersen, D. Carvey, T. Huggins, E. Peters, and B. Utgaard for lab, greenhouse, and field assistance. D. Rokhsar and J. Schmutz of DOE Joint Genome Institute provided the *M. guttatus* draft whole-genome sequence. Supported by NSF grants DEB-0316786 (L.F.) and BIO-0328326 (J. H. Willis, L.F., *et al.*). Sequences have been deposited in GenBank, with the accession numbers FJ147360 to FJ147465.

Supporting Online Material

www.sciencemag.org/cgi/content/full/322/5907/1559/DC1
 Materials and Methods
 Figs. S1 to S4
 Tables S1 and S2
 Equation S1
 References
 5 June 2008; accepted 26 September 2008
 10.1126/science.1161406

Maternal Alloantigens Promote the Development of Tolerogenic Fetal Regulatory T Cells in Utero

Jeff E. Mold,^{1,2} Jakob Michaëlsson,³ Trevor D. Burt,^{1,4} Marcus O. Muench,⁵ Karen P. Beckerman,^{6*} Michael P. Busch,⁵ Tzong-Hae Lee,⁵ Douglas F. Nixon,¹ Joseph M. McCune^{1†}

As the immune system develops, T cells are selected or regulated to become tolerant of self antigens and reactive against foreign antigens. In mice, the induction of such tolerance is thought to be attributable to the deletion of self-reactive cells. Here, we show that the human fetal immune system takes advantage of an additional mechanism: the generation of regulatory T cells (T_{regs}) that suppress fetal immune responses. We find that substantial numbers of maternal cells cross the placenta to reside in fetal lymph nodes, inducing the development of CD4+CD25^{high}FoxP3+ T_{regs} that suppress fetal antimaternal immunity and persist at least until early adulthood. These findings reveal a form of antigen-specific tolerance in humans, induced in utero and probably active in regulating immune responses after birth.

Fifty years ago, Billingham, Brent, and Medawar first advanced the concept that “actively acquired immunologic tolerance” in the mouse occurs as a result of fetal exposure to foreign antigens (1). There have since been numerous reports suggesting that the transfer of foreign antigens (including proteins, parasites, and even cells) from the mother to the fetus is a common occurrence (2–4); however, the mechanism by which the fetal immune system recognizes and responds to such antigens is unclear.

Temporal differences in the development of the adaptive immune system vary substantially between species (5). Newborn mice show few signs of peripheral T cell colonization (6), whereas in the human fetus, peripheral lymphoid tissues are populated by T cells as early as 10 gestational weeks (g.w.) (7). Therefore, it is not

clear whether in utero tolerance induction would occur upon fetal exposure to foreign antigens in the human as it does in the mouse (8). In fact, not

much is known about the functional properties of the human fetal immune system: Some reports suggest that it is functionally deficient, whereas others indicate that fetal immune responses to pathogens and vaccines are intact (9–12). In two independent clinical studies (13, 14), specific tolerance toward noninherited maternal alloantigens (NIMAs) was observed in organ transplant recipients, consistent with the possibility that fetal exposure to NIMAs may promote lasting tolerance in humans.

In certain circumstances [for example, severe combined immunodeficiency disease (15)], maternal cells cross the placenta and engraft into human fetal tissues in utero, resulting in “maternal microchimerism” (4). Because the human fetal immune system may be functionally responsive against NIMAs in utero, we wished to understand whether such microchimerism was the exception or the norm. Lymph nodes (LNs) were isolated from the mesentery of 18 fetal products of conception at 18 to 22 g.w. and analyzed for the presence of maternal DNA (16). Maternal microchimerism was observed in 15 out of 18 LN samples (Table 1 and fig. S1), with a

Table 1. Maternal microchimerism in fetal LNs. We analyzed fetal mesenteric lymph nodes (18 to 22 g.w.) for levels of maternal microchimerism with the use of two separate assays (16). Informative HLA types and/or insertion/deletion (in/del) polymorphisms are listed for each donor. “None” refers to situations where no informative HLA type or polymorphisms were identified; “Neg.” refers to samples where no microchimerism was detected; N.A., not applicable.

Sample number	HLA type/ (in/del) marker	% Microchimerism (HLA type)	% Microchimerism (in/del)
1	DR13/SO10	0.3860%	0.3080%
2	None/SO3	N.A.	0.1640%
3	DR11/None	0.8260%	N.A.
4	DR4/None	0.0035%	N.A.
5	None/None	N.A.	N.A.
6	DR9/SO7B	0.0370%	0.0906%
7	DR1/SO6	0.0650%	0.0190%
8	DR13/None	Neg.	N.A.
9	DR7/SO8	0.1780%	0.4934%
10	SO6/None	0.0062%	N.A.
11	None/SO9 SO10	N.A.	0.0070% 0.0039%
12	DR1/SO4B	0.0312%	0.0234%
13	None/SO9 SO11	N.A.	0.4869% 0.1933%
14	DR1/None	0.3663%	N.A.
15	DR15/SO3	Neg.	Neg.
16	DR11/None	0.0114%	N.A.
17	DR15/SO3	0.0161%	0.006%
18	DR15/None	0.1158%	N.A.

¹Division of Experimental Medicine, Department of Medicine, University of California at San Francisco (UCSF), San Francisco, CA 94110, USA. ²Biomedical Sciences Graduate Program, UCSF, San Francisco, CA 94143, USA. ³Center for Infectious Medicine, Department of Medicine, Karolinska University Hospital, Karolinska Institutet, 141 86, Stockholm, Sweden. ⁴Department of Pediatrics, Division of Neonatology, UCSF, San Francisco, CA 94143, USA. ⁵Blood Systems Research Institute and Department of Laboratory Medicine, UCSF, San Francisco, CA 94118, USA. ⁶Department of Obstetrics, Gynecology, and Reproductive Sciences, UCSF, San Francisco, CA 94143, USA.

*Present address: Albert Einstein College of Medicine, Bronx, NY 10461, USA.

†To whom correspondence should be addressed. E-mail: mike.mccune@ucsf.edu